Passive linearization of nonlinear resonances

G. Habib,[1] C. Grappasonni,[1] and G. Kerschen[1]
Space Structures and Systems Laboratory, Department of Aerospace and Mechanical Engineering, University of Liège, 1 Chemin des Chevreuils (B52/3), B-4000 Liège, Belgium

(Dated: 28 July 2016)

The objective of this paper is to demonstrate that the addition of properly-tuned nonlinearities to a nonlinear system can increase the range over which a specific resonance responds linearly. Specifically, we seek to enforce two important properties of linear systems, namely the force-displacement proportionality and the invariance of resonance frequencies. Numerical simulations and experiments are used to validate the theoretical findings.

PACS numbers: 05.45.-a
Keywords: nonlinear dynamics; compensation of nonlinearity; nonlinear normal modes; linearization; perturbation

Accepted manuscript. DOI: 10.1063/1.4959814

I. INTRODUCTION

Devices used for sensing, imaging and detection are usually required to exhibit linear behavior in their dynamic range. However, nonlinearity is a frequent occurrence in physical and engineering applications. For instance, in micro- and nanoresonators used for ultrasensitive force and mass sensing[1–3], radio-frequency signal processing[4], narrow band filtering[5,6], time keeping[7–9] and nanoscale imaging[10,11], nonlinear behaviors are already experienced at low amplitudes compared to the noise floor[12,13]. Nonlinearity may result in plethora of dynamic phenomena including amplitude-frequency dependence[14], modal couplings[15–17], mixed hardening-softening behaviors[12] and chaotic responses[18,19]. Clearly, these phenomena can drastically limit the performance of the devices[20,21].

One well-established approach for enforcing linear behavior is feedback linearization[22,23], which uses feedback control to cancel the undesired nonlinearities. However, feedback linearization requires an accurate monitoring of the system's states, an actuator and an external source of energy, which complicates its practical realization. There have been attempts to exploit nonlinearity rather than avoiding it. Bistability and jump phenomena were used to enhance noise squeezing[24], to enlarge the bandwidth of energy harvesters[25–28], to improve mass detection[29], to reduce the sensitivity of a resonator to the phase of the drive[7] and to develop new mechanical memory devices[30,31]. Superharmonic excitation and internal resonances were employed to improve stability properties of resonators[32] and time keeping devices[13]. Finally, the inherent frequency-energy dependence of nonlinear oscillations was exploited in broadband vibration absorbers[33].

The present paper proposes a fully passive, resonance-based approach for dealing with undesired nonlinearities in mechanical systems. Properly-tuned nonlinearities are introduced in the nonlinear system to increase the range over which a specific resonance responds linearly. Specifically, we seek to enforce two important properties of linear systems, namely the force-displacement proportionality and the invariance of resonance frequencies. Unlike previous attempts concerned with passive linearization[34,35] and manipulation of nonlinearities[36], our approach relies on a principle of similarity[37] which states that the added nonlinearity should possess the same mathematical form as that of the original nonlinear system. This principle of similarity enables us to extend the linear regime over a larger range of motion amplitudes.

II. ANALYTICAL DEVELOPMENTS

We consider an n-degree-of-freedom (DoF) mechanical system with concentrated nonlinearities subject to harmonic excitation:

$$\tilde{\mathbf{M}}\ddot{\mathbf{x}} + \tilde{\mathbf{C}}\dot{\mathbf{x}} + \tilde{\mathbf{K}}\mathbf{x} + \tilde{\mathbf{b}}_{nl}(\mathbf{x}) = \sqrt{\varepsilon}\tilde{\mathbf{v}} f \cos\omega t, \qquad (1)$$

where ε is a small bookkeeping parameter. $\tilde{\mathbf{M}}$, $\tilde{\mathbf{C}}$ and $\tilde{\mathbf{K}}$ are the mass, damping and stiffness matrices, respectively, $\sqrt{\varepsilon}\tilde{\mathbf{v}} f \cos\omega t$ is the forcing term and $\mathbf{x}$ is the position vector. The vector $\tilde{\mathbf{b}}_{nl}(\mathbf{x})$ contains both the original and additional nonlinearities, which are of polynomial nature. According to the principle of similarity[37], the additional nonlinearities should possess the same exponent as the original nonlinearity. Without loss of generality, cubic nonlinearities are considered herein.

The objective of this study is to linearize one specific resonance of system (1) through the proper design of the additional nonlinearities. To this end, the nonlinear normal mode (NNM) theory is exploited, because nonlinear resonances are known to occur in the neighborhood of NNMs[38]. First, we transform Eq. (1) into modal space through the change of variables $\mathbf{x} = \mathbf{U}\mathbf{y}$ where $\mathbf{U}$ contains the normal modes of the underlying linear system, and we define normalized modal displacements, $\mathbf{q} = \mathbf{y}/(\sqrt{\varepsilon} f)$, such that

$$\ddot{\mathbf{q}} + \mathbf{C}\dot{\mathbf{q}} + \mathbf{\Omega}\mathbf{q} + \mathbf{b}_{nl}(x) = \mathbf{v}\cos\omega t, \qquad (2)$$

where $\mathbf{\Omega} = \text{diag}\left[\Omega_j^2\right]_{j=\overline{1,n}}$, $\mathbf{C} = \left[c_{ij}\right]_{i,j=\overline{1,n}}$ and

$$\mathbf{b}_{nl}\left(\mathbf{x}\right) = \begin{bmatrix} \vdots \\ \varepsilon f^2 \sum_{h_1+\ldots+h_n=3} b_{jh_1\ldots h_n} \prod_{i=1}^{n} q_i^{h_i} \\ \vdots \end{bmatrix}. \quad (3)$$

$\mathbf{b}_{nl}\left(\mathbf{x}\right)$ is the projection of $\tilde{\mathbf{b}}_{nl}\left(\mathbf{x}\right)$ in modal space, thus, even if $\tilde{\mathbf{b}}_{nl}\left(\mathbf{x}\right)$ is sparse, $\mathbf{b}_{nl}\left(\mathbf{x}\right)$ can be fully populated. $b_{jh_1\ldots h_n}$ are scalars, where j indicates the mode number and varies according to the rows of $\mathbf{b}_{nl}\left(\mathbf{x}\right)$, while subscripts $h_1 \ldots h_n$ are in accordance with the exponents of the modal coordinates of the corresponding terms. We assume that the system features no internal resonances, i.e., natural frequencies Ω_j are incommensurate.

The NNMs are now calculated by removing damping and forcing terms in Eq. (2). Following a standard perturbation technique and limiting the solution to the fundamental harmonic, the approximate solution has the form

$$\mathbf{q} = \left(\mathbf{q}_0 + \varepsilon\mathbf{q}_1 + O\left(\varepsilon^2\right)\right)\sin\left(\left(\omega_0 + \varepsilon\omega_1 + O\left(\varepsilon^2\right)\right)t\right), \quad (4)$$

where $\mathbf{q}_0 = \left[\cdots, q_{j0}, \cdots\right]^{\mathrm{T}}$ and $\mathbf{q}_1 = \left[\cdots, q_{j1}, \cdots\right]^{\mathrm{T}}$. We adopt the standard single harmonic approximation $\sin^3\left(\omega t\right) \approx 3/4 \sin\left(\omega t\right)$. Imposing resonance condition at order ε^0 and solving terms of order ε^1 yields for the l^{th} NNM

$$q_{j0} = 0,\ q_{j1} = -\frac{3}{4}\frac{b_{j0\ldots3\ldots0}q_{l0}^3}{\Omega_j^2 - \Omega_l^2} \quad \text{for } j = \overline{1,n},\ j \neq l, \quad (5)$$

$$\omega_0 = \Omega_l,\ \omega_1 = \frac{3}{4}\frac{b_{l0\ldots3\ldots0}q_{l0}^2}{2\Omega_l}. \quad (6)$$

q_{j0} and q_{j1} $(j \neq l)$ represent the influence of the nonresonant modes on the l^{th} mode. ω_1 is the variation of the l^{th} natural frequency with respect to the amplitude of oscillation q_{l0}. Thus, if $b_{l0\ldots3\ldots0} > 0$ (< 0), the resonance is of hardening (softening) type.

In order to relate the undamped, unforced NNM motions to the resonances of the damped, forced system, the energy balance criterion[39] is utilized:

$$\int_0^T \dot{\mathbf{q}}(t)^{\mathrm{T}}\mathbf{C}\dot{\mathbf{q}}(t)\mathrm{d}t = \int_0^T \dot{\mathbf{q}}(t)^{\mathrm{T}}\mathbf{v}\cos\omega t\,\mathrm{d}t, \quad (7)$$

where T is the period of motion. Eq. (7) indicates that at resonance the energy dissipated by damping over a full period is equal to the input energy. Inserting the approximate solution for $\mathbf{q}$ in Eq. (7) gives

$$q_{l0} = \frac{v_l}{\Omega_l c_{ll}}, \quad (8)$$

$$q_{l1} = \frac{\Omega_l q_{l0}\left(\sum_{\substack{j=1\\j\neq l}}^{n} c_{lj}q_{j1} + \sum_{\substack{j=1\\j\neq l}}^{n} c_{jl}q_{j1}\right) - \sum_{\substack{j=1\\j\neq l}}^{n} q_{j1}v_j}{v_l - 2\Omega_l q_{l0}c_{ll}} + \frac{\omega_1 q_{l0}^2 c_{ll}}{v_l - 2\Omega_l q_{l0}c_{ll}}. \quad (9)$$

and

$$x_k = \sqrt{\varepsilon}f\left(u_{kl}q_{l0} + \varepsilon\left(\sum_{j=1}^{n} u_{kj}q_{j1}\right) + O\left(\varepsilon^2\right)\right). \quad (10)$$

Eqs. (5), (6), (8), (9) and (10) completely define the l^{th} resonance of system (1) and form the basis of the design procedure developed in this work. Based on these equations, force-displacement proportionality for coordinate x_k of the l^{th} resonance can simply be enforced through

$$\sum_{j=1}^{n} u_{kj}q_{j1} = 0. \quad (11)$$

Indeed, if this latter condition is fulfilled, Eq. (10) transforms into

$$x_k \approx \sqrt{\varepsilon}f u_{kl}q_{l0}. \quad (12)$$

Similarly, invariance of the l^{th} resonance frequency can be enforced through

$$\omega_1 = 0, \quad (13)$$

such that the l^{th} natural frequency $\omega_l \approx \omega_0$.

Since Eqs. (11) and (13) involve the n coefficients of the nonlinear terms $b_{j0\ldots3\ldots0}$, they can be used to design the additional nonlinearities in function of the original ones.

III. EXPERIMENTAL VALIDATION

A. Force-displacement proportionality

Two different experimental systems are utilized to demonstrate the proposed idea. The first one, pictured in Fig. 1, comprises a 700 mm long cantilever beam (cross section 14x14 mm), made of steel to which a 240 mm long doubly-clamped beam, built using 3D printing, is connected. The doubly-clamped beam is supported by a thick frame assumed rigid, moreover, a small mass is placed in the middle of its span in order to reduce its principal natural frequency. The input force is applied to the cantilever beam using an electrodynamic shaker. The shaker excites the structure in the x direction, according to the coordinate reference included in Fig. 1. The original nonlinearity in this coupled system is due to a thin steel lamina located at the free end of the cantilever beam (cross section 14x0.5 mm, see Fig. 1) whereas the additional nonlinearity comes from the doubly-clamped beam itself. The nonlinearities are of geometric nature and are activated for sufficiently large motion amplitudes. Both of them can be modeled using cubic springs, which satisfies the principle of similarity.

The frequency range encompassing only the first two modes of vibration was considered. Their shapes are qualitatively represented in Fig. 2.

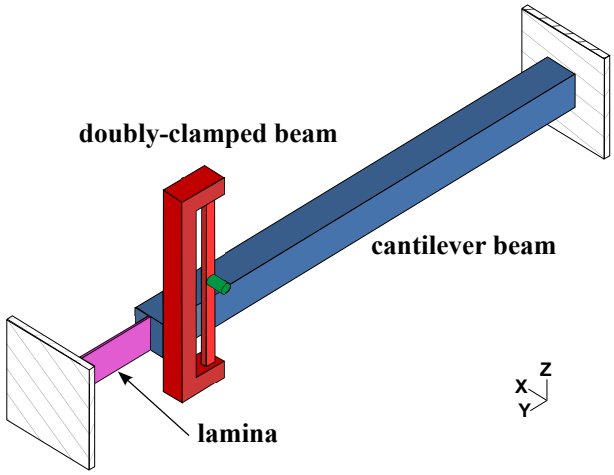

FIG. 1. Schematic representation of the experimental set-up for enforcing force-displacement proportionality.

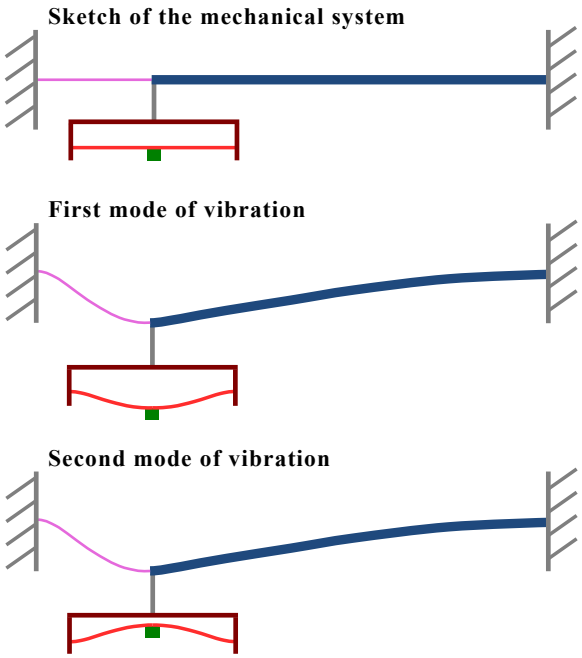

FIG. 2. Schematic representation of the first two modes of vibration of the mechanical system. The doubly-clamped beam is rotated for a better visualization.

A two-DoF reduced model of the system without the additional nonlinearity was first identified experimentally

$$\begin{aligned} &0.46\ddot{x}_1 + 0.52\dot{x}_1 - 0.15\dot{x}_2 + 14065x_1 - 1710x_2 \\ &\quad + 3.3\times10^9 x_1^3 = f\cos\omega t \\ &0.07\ddot{x}_2 - 0.15\dot{x}_1 + 0.25\dot{x}_2 + 1710(x_2 - x_1) = 0. \end{aligned} \tag{14}$$

where 3.3×10^9 N/m^3 is the nonlinear coefficient of the steel lamina. The reduced model was then used to compute nonlinear frequency responses for harmonic excitation of amplitudes f up to 0.5 N. Fig. 3a illustrates that the second resonance is significantly distorted by the nonlinearity of the steel lamina; it is therefore the target resonance in this study.

To enforce force-displacement proportionality for this resonance, the nonlinearity of the doubly-clamped beam is now considered:

$$\begin{aligned} &0.46\ddot{x}_1 + 0.52\dot{x}_1 - 0.15\dot{x}_2 + 14065x_1 - 1710x_2 \\ &\quad + 3.3\times10^9 x_1^3 + k_{nl2}\left(x_1 - x_2\right)^3 = f\cos\left(\omega t\right) \\ &0.07\ddot{x}_2 - 0.15\dot{x}_1 + 0.25\dot{x}_2 + 1710(x_2 - x_1) \\ &\quad + k_{nl2}\left(x_2 - x_1\right)^3 = 0. \end{aligned} \tag{15}$$

The adequate nonlinear coefficient can be determined using Eq. (11), i.e. $k_{nl2} = 4.27\times10^7$ N/m^3. The numerical simulations in Fig. 3b confirm that the second resonance obeys force-displacement proportionality, which validates our theoretical developments.

The cross section of the doubly-clamped beam was thus designed so as to achieve the requested value for k_{nl2}, according to the formula[40] $k_{nl2} = 3k_2/\left(4t^2\right)$, where t is the thickness of the doubly-clamped beam, and k_2 is its linear stiffness. Because of the uncertainties inherent to 3D printing, the value identified experimentally for k_{nl2} was 3.8×10^7 N/m^3.

The second resonance with the additional nonlinearity was measured experimentally for 8 forcing amplitudes up to 0.3 N (greater forcing amplitudes induced significant shaker-structure interactions). The corresponding peak amplitudes are represented by red circles in Fig. 3c. Because the circles are almost aligned horizontally, one can conclude that the displacement of the experimental cantilever beam around the second resonance is proportional to the amplitude of the harmonic forcing. For comparison, the results of numerical simulations are superposed in Fig. 3c. The solid line ($k_{nl2} = 3.8\times10^7$ N/m^3) indicates that an excellent agreement between experimental and numerical results is obtained. The dashed line ($k_{nl2} = 0$ N/m^3) shows the significant variation of the peak amplitude with the forcing level before the addition of the intentional nonlinearity. Another finding is that, in spite of the 11% difference between the theoretical and actual nonlinearity of the doubly-clamped beam, force-displacement proportionality was enforced quite accurately in the experiment, which shows the robustness of our procedure. Furthermore, extensive numerical analyses of the basins of attraction of the system did not show the existence of any other stable solution.

B. Isochronicity

The second experimental system, pictured in Fig. 4, comprises the same cantilever beam to which another doubly-clamped beam is connected. The system has two hardening nonlinearities, one due to the thin steel lamina and one due to the doubly-clamped beam itself. A two-DoF reduced order model of the system was identified

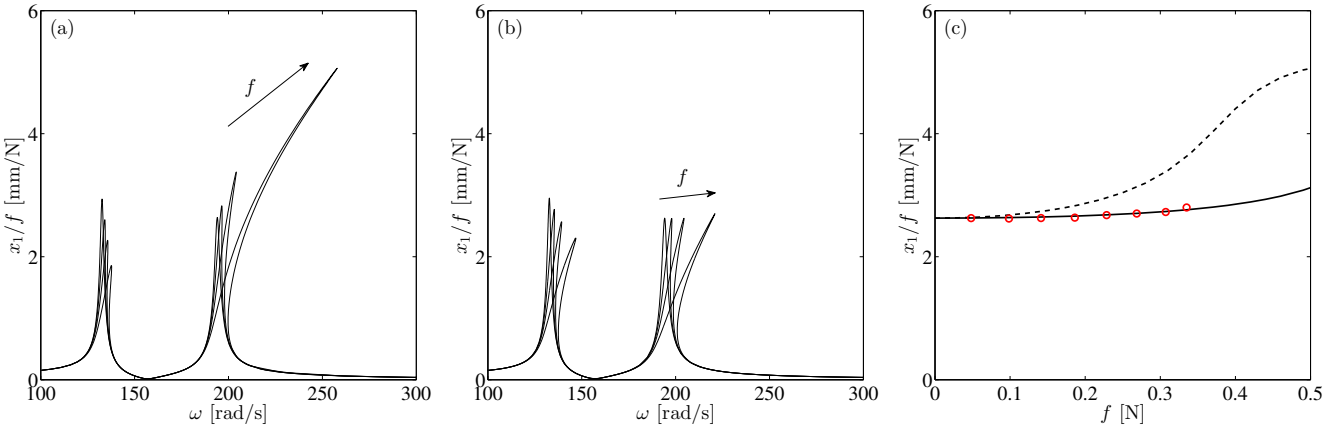

FIG. 3. (a,b) Numerical frequency responses of the 2 DoF beam model in Eq. (15) for $f = 0.048, 0.186, 0.307, 0.50$ N. (a) $k_{nl2} = 0$ N/m^3 and (b) $k_{nl2} = 4.27 \times 10^7$ N/m^3. (c) Second resonant peak for increasing forcing amplitudes; red circles: experimental results, dashed line: $k_{nl2} = 0$ N/m^3 and solid line: $k_{nl2} = 3.8 \times 10^7$ N/m^3.

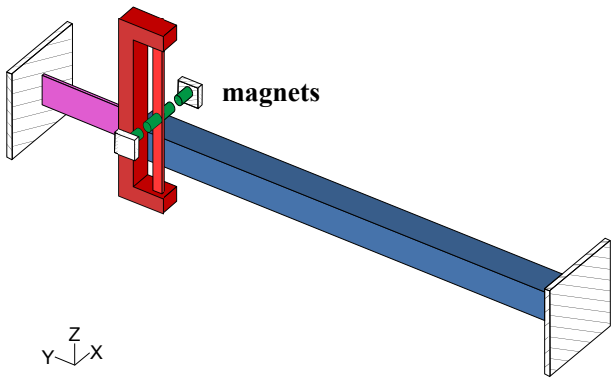

FIG. 4. Schematic representation of the experimental set-up for enforcing invariance of resonance frequency.

experimentally

$$\begin{aligned} &0.36\ddot{x}_1 + 0.005\ddot{x}_2 + 0.25\dot{x}_1 - 0.3\dot{x}_2 + 10495x_1 - 3447x_2 \\ &\quad + 2 \times 10^9 x_1^3 + 8 \times 10^7 (x_1 - x_2)^3 = f \cos \omega t \\ &0.005\ddot{x}_1 + 0.058\ddot{x}_2 - 0.3\dot{x}_1 + 0.54\dot{x}_2 + 3447 (x_2 - x_1) \\ &\quad + 8 \times 10^7 (x_2 - x_1)^3 = 0. \end{aligned} \tag{16}$$

The numerical frequency responses around the first resonance are represented in Fig. 5a. The resonance frequency undergoes a significant variation due to the hardening nonlinearities.

In order to compensate this frequency shift, a couple of permanent magnets was attached directly to the doubly-clamped beam. Additional magnets fixed on an external support were placed symmetrically with a gap d, as illustrated in Fig. 4b. The two pairs of magnets are mutually attractive. The full system dynamics is described by

$$\begin{aligned} &0.36\ddot{x}_1 + 0.005\ddot{x}_2 + 0.25\dot{x}_1 - 0.3\dot{x}_2 + 10495x_1 - 3447x_2 \\ &\quad + 2 \times 10^9 x_1^3 + 8 \times 10^7 (x_1 - x_2)^3 = f \cos \omega t \\ &0.005\ddot{x}_1 + 0.058\ddot{x}_2 - 0.3\dot{x}_1 + 0.54\dot{x}_2 + 3447 (x_2 - x_1) \\ &\quad + k_3 x_2 + 8 \times 10^7 (x_2 - x_1)^3 + k_{nl3} x_2^3 = 0, \end{aligned} \tag{17}$$

where k_3 and k_{nl3} are the linear and cubic coefficients of the magnetic force, respectively. These coefficients were estimated analytically[41]. Their value is negative (softening) and depends on the reciprocal distance d between the magnets, as shown by the dashed line in Fig. 6.

Isochronicity for the first resonance can now be enforced through Eq. (13), and the result is the solid line in Fig. 6. The intersection of the solid and dashed lines therefore indicates that the magnets should have a reciprocal distance of 4.4 mm, which results in $k_3 = -1160$ N/m and $k_{nl3} = -1.26 \times 10^8$ N/m^3. Due to unavoidable positioning error, the coefficients of the experimental system were measured to be $k_3 = -1000$ N/m and $k_{nl3} = -1 \times 10^8$ N/m^3, which correspond to a distance $d = 4.6$ mm.

The experimental results are represented by red circles in Fig. 5b; the resonance frequency seems to be almost constant (very slightly softening), which validates our methodology. The numerical results superposed in Fig. 5b also evidence the excellent predictive capability of the developed reduced-order model of the set-up. Also in this case, no additional stable solution was evidenced by numerical analyses of the basins of attraction.

IV. CONCLUSIONS

In this paper, we demonstrated using supporting analytical, numerical and experimental results that it is

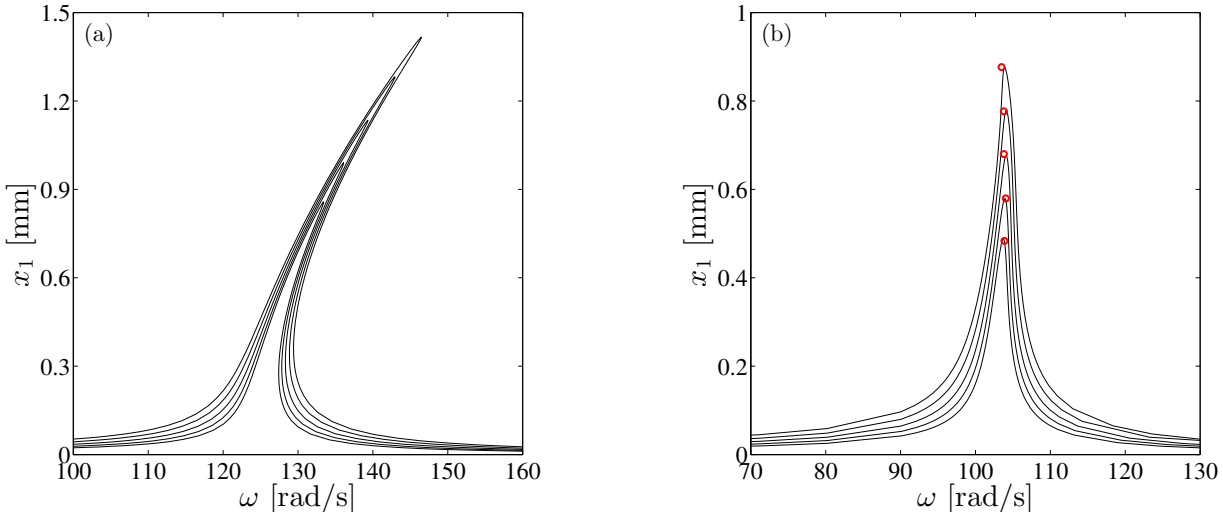

FIG. 5. Frequency responses of the 2 DoF beam model in Eq. (17) for $f = 0.060$, 0.074, 0.092, 0.114, 0.138 N. (a) $k_3 = k_{nl3} = 0$ and (b) $k_3 = -1000$ N/m and $k_{nl3} = -1 \times 10^8$ N/m^3. Red circles: experimental results, and solid lines: numerical simulations.

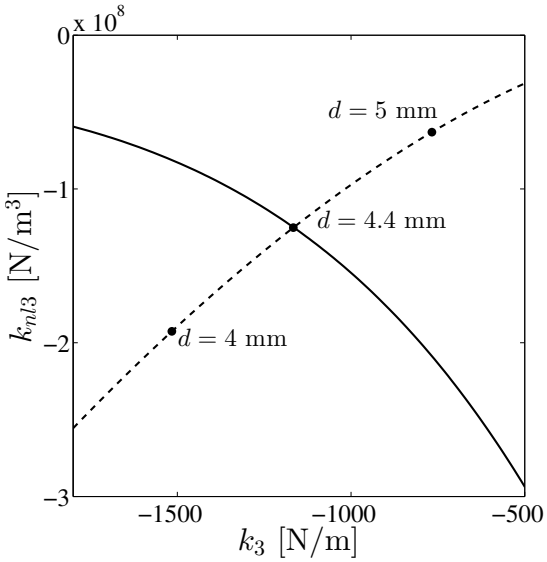

FIG. 6. Magnets design. Solid line: isochronicity condition; dashed line: magnetic force coefficients as a function of the magnets relative distance.

possible to linearize a specific resonance of a nonlinear system through the addition of intentional nonlinearities. Our methodology, which relies on a principle of similarity between the added and original nonlinearities, paves the way for performance improvement of existing engineering devices, for instance, by enlarging the dynamic range in which these devices exhibit linear-like behaviors. If the proposed procedure can find applications in macroscopic mechanical structures, it is particularly suitable for micro- and nano-resonators, which are known to experience nonlinear behaviors already at low amplitudes.

ACKNOWLEDGEMENT

The authors would like to acknowledge the financial support of the European Union (ERC Starting Grant NoVib 307265).

[1] M. D. Dai, K. Eom, and C.-W. Kim, "Nanomechanical mass detection using nonlinear oscillations," Applied Physics Letters **95**, 203104 (2009).
[2] B. Lassagne, D. Ugnati, and M. Respaud, "Ultrasensitive magnetometers based on carbon-nanotube mechanical resonators," Physical Review Letters **107**, 130801 (2011).
[3] V. Kumar, J. W. Boley, Y. Yang, H. Ekowaluyo, J. K. Miller, G. T.-C. Chiu, and J. F. Rhoads, "Bifurcation-based mass sensing using piezoelectrically-actuated microcantilevers," Applied Physics Letters **98**, 153510 (2011).
[4] C. T. Nguyen, "Frequency-selective mems for miniaturized low-power communication devices," Microwave Theory and Techniques, IEEE Transactions on **47**, 1486–1503 (1999).
[5] S.-J. Park, I. Reines, C. Patel, and G. M. Rebeiz, "High-rf-mems 4–6-ghz tunable evanescent-mode cavity filter," Microwave Theory and Techniques, IEEE Transactions on **58**, 381–389 (2010).
[6] S. Fouladi, F. Huang, W. D. Yan, and R. R. Mansour, "High-narrowband tunable combline bandpass filters using mems capacitor banks and piezomotors," Microwave Theory and Techniques, IEEE Transactions on **61**, 393–402 (2013).
[7] B. Yurke, D. Greywall, A. Pargellis, and P. Busch, "Theory of amplifier-noise evasion in an oscillator employing a nonlinear resonator," Physical Review A **51**, 4211 (1995).
[8] C. T.-C. Nguyen, "Mems technology for timing and frequency control," Ultrasonics, Ferroelectrics, and Frequency Control, IEEE Transactions on **54**, 251–270 (2007).
[9] D. Antonio, D. A. Czaplewski, J. R. Guest, D. López, S. I. Arroyo, and D. H. Zanette, "Nonlinearity-induced synchronization enhancement in micromechanical oscillators," Physical Review Letters **114**, 034103 (2015).
[10] G. Binnig, C. F. Quate, and C. Gerber, "Atomic force microscope," Physical Review Letters **56**, 930 (1986).
[11] M. Korayem and N. Ebrahimi, "Nonlinear dynamics of tapping-mode atomic force microscopy in liquid," Journal of Applied Physics **109**, 084301 (2011).

[12]N. Kacem and S. Hentz, "Bifurcation topology tuning of a mixed behavior in nonlinear micromechanical resonators," Applied Physics Letters **95**, 183104 (2009).
[13]D. Antonio, D. H. Zanette, and D. López, "Frequency stabilization in nonlinear micromechanical oscillators," Nature communications **3**, 806 (2012).
[14]M. Agarwal, S. A. Chandorkar, H. Mehta, R. N. Candler, B. Kim, M. A. Hopcroft, R. Melamud, C. M. Jha, G. Bahl, G. Yama, *et al.*, "A study of electrostatic force nonlinearities in resonant microstructures," Applied Physics Letters **92**, 4106 (2008).
[15]H. Westra, M. Poot, H. Van Der Zant, and W. Venstra, "Nonlinear modal interactions in clamped-clamped mechanical resonators," Physical Review Letters **105**, 117205 (2010).
[16]G. Tancredi, G. Ithier, and P. Meeson, "Bifurcation, mode coupling and noise in a nonlinear multimode superconducting microwave resonator," Applied Physics Letters **103**, 063504 (2013).
[17]P. Truitt, J. Hertzberg, E. Altunkaya, and K. Schwab, "Linear and nonlinear coupling between transverse modes of a nanomechanical resonator," Journal of Applied Physics **114**, 114307 (2013).
[18]D. L. Gonzalez and O. Piro, "Chaos in a nonlinear driven oscillator with exact solution," Physical Review Letters **50**, 870 (1983).
[19]P. Berggren and J. Fransson, "Stability and chaos of a driven nanoelectromechanical josephson junction," Physical Review B **85**, 195439 (2012).
[20]H. C. Postma, I. Kozinsky, A. Husain, and M. Roukes, "Dynamic range of nanotube-and nanowire-based electromechanical systems," Applied Physics Letters **86**, 223105 (2005).
[21]O. Thomas, F. Mathieu, W. Mansfield, C. Huang, S. Trolier-McKinstry, and L. Nicu, "Efficient parametric amplification in micro-resonators with integrated piezoelectric actuation and sensing capabilities," Applied Physics Letters **102**, 163504 (2013).
[22]S. Mittal and C.-H. Menq, "Precision motion control of a magnetic suspension actuator using a robust nonlinear compensation scheme," Mechatronics, IEEE/ASME Transactions on **2**, 268–280 (1997).
[23]B. Charlet, J. Lévine, and R. Marino, "On dynamic feedback linearization," Systems & Control Letters **13**, 143–151 (1989).
[24]R. Almog, S. Zaitsev, O. Shtempluck, and E. Buks, "Noise squeezing in a nanomechanical duffing resonator," Physical Review Letters **98**, 078103 (2007).
[25]G. Kopidakis, S. Aubry, and G. Tsironis, "Targeted energy transfer through discrete breathers in nonlinear systems," Physical Review Letters **87**, 165501 (2001).
[26]F. Cottone, H. Vocca, and L. Gammaitoni, "Nonlinear energy harvesting," Physical Review Letters **102**, 080601 (2009).
[27]S. C. Stanton, C. C. McGehee, and B. P. Mann, "Reversible hysteresis for broadband magnetopiezoelastic energy harvesting," Applied Physics Letters **95**, 174103 (2009).
[28]K. Fan, J. Chang, W. Pedrycz, Z. Liu, and Y. Zhu, "A nonlinear piezoelectric energy harvester for various mechanical motions," Applied Physics Letters **106**, 223902 (2015).
[29]M. I. Younis and F. Alsaleem, "Exploration of new concepts for mass detection in electrostatically-actuated structures based on nonlinear phenomena," Journal of computational and nonlinear dynamics **4**, 021010 (2009).
[30]H. Noh, S.-B. Shim, M. Jung, Z. G. Khim, and J. Kim, "A mechanical memory with a dc modulation of nonlinear resonance," Applied Physics Letters **97**, 033116 (2010).
[31]N. Khovanova and J. Windelen, "Minimal energy control of a nanoelectromechanical memory element," Applied Physics Letters **101**, 024104 (2012).
[32]N. Kacem, S. Baguet, R. Dufour, and S. Hentz, "Stability control of nonlinear micromechanical resonators under simultaneous primary and superharmonic resonances," Applied Physics Letters **98**, 193507 (2011).
[33]O. Gendelman, L. Manevitch, A. F. Vakakis, and R. Mcloskey, "Energy pumping in nonlinear mechanical oscillators: Part i–dynamics of the underlying hamiltonian systems," Journal of Applied Mechanics **68**, 34–41 (2001).
[34]I. Kozinsky, H. C. Postma, I. Bargatin, and M. Roukes, "Tuning nonlinearity, dynamic range, and frequency of nanomechanical resonators," Applied Physics Letters **88**, 253101 (2006).
[35]I. Kovacic and R. Rand, "About a class of nonlinear oscillators with amplitude-independent frequency," Nonlinear Dynamics **74**, 455–465 (2013).
[36]S. Dou, B. S. Strachan, S. W. Shaw, and J. S. Jensen, "Structural optimization for nonlinear dynamic response," Philosophical Transactions of the Royal Society A **373**, 20140408 (2015).
[37]G. Habib and G. Kerschen, "A principle of similarity for nonlinear vibration absorbers," Physica D: Nonlinear Phenomena **332**.
[38]A. F. Vakakis, L. I. Manevitch, Y. V. Mikhlin, V. N. Pilipchuk, and A. A. Zevin, *Normal modes and localization in nonlinear systems* (Springer, 1996).
[39]T. Hill, A. Cammarano, S. Neild, and D. Wagg, "An analytical method for the optimisation of weakly nonlinear systems," Proceedings of EURODYN 2014 , 1981–1988 (2014).
[40]S. D. Senturia, *Microsystem design* (Springer Science & Business Media, 2007).
[41]D. Vokoun, M. Beleggia, L. Heller, and P. Šittner, "Magnetostatic interactions and forces between cylindrical permanent magnets," Journal of Magnetism and Magnetic Materials **321**, 3758–3763 (2009).